Journal of
Mechanics of Materials and Structures

ESTIMATION OF PARAMETERS OF A THREE-LAYERED SANDWICH BEAM

Nilson Barbieri, Renato Barbieri, Luiz Carlos Winikes and Luis Fernando Oresten

Volume 3, Nº 3 *March 2008*

mathematical sciences publishers

JOURNAL OF MECHANICS OF MATERIALS AND STRUCTURES
Vol. 3, No. 3, 2008

ESTIMATION OF PARAMETERS OF A THREE-LAYERED SANDWICH BEAM

NILSON BARBIERI, RENATO BARBIERI, LUIZ CARLOS WINIKES AND LUIS FERNANDO ORESTEN

In this work the physical parameters of a sandwich beam made with the association of hot rolled steel, polyurethane rigid foam, and high impact polystyrene, used for the assembly of household refrigerators and food freezers, are estimated using measured and numeric frequency response functions. The mathematical models are obtained using the finite element method and the Timoshenko beam theory. The physical parameters are estimated using the amplitude correlation coefficient and genetic algorithm methods. Initially, the experimental procedure to determine the material's mechanical properties, Young and shear moduli, and the density of the components of the sandwich beam is described. The elastic properties were obtained through tension and torsion tests. The shear modulus G_c of the polyurethane rigid foam core was determined using a rectangular specimen and the Young's moduli of the steel and high impact polystyrene were determined using a conventional tension test. To estimate the dynamical values of the parameters in the frequency range from 10 to 400 Hz, separated dynamic sweeping tests were conducted using cantilevered beams of polyurethane rigid foam and high impact polystyrene. The experimental data from a three layered sandwich beam were obtained using an impact hammer and four accelerometers, displaced along the cantilevered beam sample. The parameters estimated are the Shear modulus and the loss factor of the polyurethane rigid foam, and the Young's modulus and the loss factor of the high impact polystyrene.

1. Introduction

Modern engineering requires the use of sophisticated and optimized structural designs. One way to achieve this goal is to use materials in a way that will optimize their inherent properties. An engineering application known as sandwich structure is very suitable for this purpose. Sandwich materials are frequently used wherever high strength and low weight are important criteria. The most important applications are found in the transport industry — such as in the aerospace, automobile, railroad, and marine industries — where high stiffness/weight and strength/weight ratios provide increased payload capacity, improved performance, and lower energy consumption. These applications are often subjected to vibrations. It is therefore important to know the particular dynamic and vibroacoustic properties, such as the natural frequencies, of these constructions for design purposes [Tavallaey 2001].

For household refrigerators and food freezers, one of the main complaints to customer care centers is related to noise generation, related most of the time to vibration of the cabinet, which radiates sound from internal components like shelves and containers, leaking to the outside of the unit.

The modeling of sandwich structures has been studied extensively, but less attention has been paid to their material identification [Shi et al. 2006]. Material parameter identification by inverse methods

Keywords: sandwich beam, genetic algorithm, amplitude correlation coefficient, parameter updating.

using measured resonance frequencies is a recent type of nondestructive evaluation method. The principle of inverse methods for material identification is to update iteratively the engineering constants in a finite element model of the test specimens in such a way that the computed frequencies match the measured frequencies. The engineering constants that minimize an output residual are considered as the solution of the procedure. The minimization of the output residual is realized by optimization methods, which minimize a scalar value called the objective function. A typical objective function is the sum of the squared residual components. The underlying idea of inverse methods based on measurement of resonance frequencies originates from the observation that all constructions made with elastic materials have a characteristic set of resonance frequencies. The values of these frequencies are determined by the geometry, boundary conditions, the elastic moduli, and the density of the materials.

Caracciolo et al. [2004] presented an experimental technique for completely characterizing a viscoelastic material, by determining the Poisson's ratio and the complex dynamic Young's modulus of a small beam-like specimen subject to seismic excitation, together with the theoretical background. The same experimental device is used basically for both kinds of tests; the specimen is instrumented, placed into a temperature controlled chamber and excited by means of an electrodynamic shaker. The longitudinal and the transversal deformations are measured by strain gauges to get the Poisson's ratio, whereas the vertical displacement of the specimen and the acceleration of the support are measured to get Young's modulus of the tested material. The experimental curves of the Poisson's ratio and of the Young's modulus, obtained at different temperatures, are then gathered into a unique master curve by using the reduced variables method. The two master curves, respectively, represent the Poisson's ratio and Young's modulus for the tested material in a very broad frequency range.

Park [2005] used experimental methods to measure frequency-dependant dynamic properties of complex structures. Flexural wave propagations are analyzed using the Timoshenko beam, the classical beam, and the shear beam theories. Wave speeds, bending, and shear stiffnesses of the structures are measured through the transfer function method, requiring small number of vibration measurements. Sensitivity analysis is performed to investigate the effects of experimental variables on the measured properties and to study optimal sensor locations of the vibration measurements. Using the developed methods, the complex bending and shear stiffnesses of sandwich beams of different core materials and a polymer beam are measured. Continuous variations of the measured bending and shear stiffnesses and their loss factors with frequency were obtained. To further illustrate the measurements of frequency-dependent variation of dynamic properties of complex structures, the damping of structural vibration using porous and granular materials is investigated.

Kim and Kreider [2006] studied the parameter identification in nonlinear elastic and viscoelastic plates by solving an inverse problem numerically. The material properties of the plate, which appear in the constitutive relations, are recovered by optimizing an objective function constructed from reference strain data. The resulting inverse algorithm consists of an optimization algorithm coupled with a corresponding direct algorithm that computes the strain fields given a set of material properties. Numerical results are presented for a variety of constitutive models; they indicate that the methodology works well, even with noisy data.

Pintelon et al. [2004] analyzed the stress-strain relationship of linear viscoelastic materials characterized by a complex valued, frequency-dependent elastic modulus (Young's modulus). Using system identification techniques it is shown the elastic modulus can be measured accurately in a broad frequency

band from forced flexural (transverse) and longitudinal vibration experiments on a beam under free-free boundary conditions. The approach is illustrated on brass, copper, plexiglass, and PVC beams.

Yang et al. [2005] analyzed the vibration and dynamic stability of a traveling sandwich beam using the finite element method. The damping layer is assumed to be linear viscoelastic and almost incompressible. The extensional and shear moduli of the viscoelastic material are characterized by complex quantities. Complex eigenvalue problems are solved by the state-space method, and the natural frequencies and modal loss factors of the composite beam are extracted. The effects of stiffness and thickness ratios of the viscoelastic and constrained layers on natural frequencies and modal loss factors are reported. Tension fluctuations are the dominant source of excitation in a traveling sandwich material, and the regions of dynamic instability are determined by a modified Bolotin's method. Numerical results show that the constrained damping layer stabilizes the traveling sandwich beam.

Singh et al. [2003] formulated a system identification procedure for estimation of parameters associated with a dynamic model of a single degree of freedom foam-mass system. Ohkami and Swoboda [1999] presented two parameter identification procedures for linear viscoelastic materials. Chang [2006] used the genetic algorithm for parameter estimation of nonlinear systems.

Backström and Nilsson [2007] indicate the need for simple methods describing the dynamics of these complex structures. By implementing frequency dependent parameters, the vibration of sandwich composite beams can be approximated using simple fourth order beam theory. A higher order sandwich beam model is utilized in order to obtain estimates of the frequency-dependent bending stiffness and shear modulus of the equivalent Euler–Bernoulli and Timoshenko models. The resulting predicted eigenfrequencies and transfer accelerance functions are compared to the data obtained from the higher order model and from measurements. It can be noticed that for lower order wavenumbers the ordinary Timoshenko theory and the higher order theory show satisfactory agreement.

In this work the physical parameters of a sandwich beam made with the association of hot rolled steel, polyurethane rigid foam, and high impact polystyrene, used for the assembly of household refrigerators and food freezers, are estimated using measured and numeric frequency response functions (FRFs). The mathematical models are obtained using the finite element method (FEM) and Timoshenko beam theory. The physical parameters are estimated using the amplitude correlation coefficient [Grafe 1998] and genetic algorithm (GA) [Chang 2006] methods. The experimental data are obtained using an impact hammer and four accelerometers displaced along the cantilevered beam sample. The parameters estimated are the shear modulus and the loss factor of the polyurethane rigid foam and the Young's modulus and the loss factor of the high impact polystyrene. The frequency range is chosen for the test in which the FRF curve presents a good signal to noise ratio. To estimate the initial values of the parameters, separated static and dynamic tests were conducted using cantilevered beams of polyurethane rigid foam and high impact polystyrene. The static values are used as the initial reference values for the dynamic estimation.

2. Mathematical model

A lot of research has been done on finite element models of cantilever beams based on Euler–Bernoulli beam theory. In Euler–Bernoulli beam theory the assumption is made that the plane cross section before bending remains plane and normal to the neutral axis after bending. This assumption is valid if the

length to thickness ratio is large, and for small deflection of beam. However if the length to thickness ratio is small, plane deflection before bending will not remain normal to the neutral axis after bending. In practical situations a large number of modes of vibrations contribute to the structure's performance. Euler–Bernoulli beam theory gives inaccurate results for higher modes of vibration. Timoshenko beam theory corrects the simplifying assumptions made in Euler–Bernoulli beam theory. In this theory cross sections remain plane and rotate about the same neutral axis as the Euler–Bernoulli model, but do not remain normal to the deformed longitudinal axis. The deviation from normality is produced by a transverse shear that is assumed to be constant over the cross section. Thus the Timoshenko beam model is superior to the Euler–Bernoulli model in precisely predicting the beam response [Backström and Nilsson 2007] for a lower number of vibration modes.

The equation of motion for the vibration of a sandwich beam according to the Timoshenko beam theory [Zenkert 1997] is

$$D\frac{\partial^4 w}{\partial x^4}+\rho^*\frac{\partial^2 w}{\partial t^2}-\frac{\rho^*}{S}\left(D\frac{\partial^4 w}{\partial x^2\partial t^2}-\Re\frac{\partial^4 w}{\partial t^4}\right)-\Re\frac{\partial^4 w}{\partial x^2\partial t^2}=f(x)e^{i\omega t}, \tag{1}$$

where $w(x,t)$ is the transverse displacement, D is the bending stiffness, ρ^* is the mass per unit of surface, S is the shear stiffness, $\Re$ is the rotational inertia, x is the coordinate along the beam axis, t is the time, $f(x)$ is the amplitude of the external force applied along the beam span, ω is the excitation frequency, and $i=\sqrt{-1}$.

The dimensions and parameters of the sandwich beam shown in Figure 1 are as follows: E_1, E_2, and E_c are the Young's moduli, ρ_1, ρ_2, and ρ_c are the densities, G_c is the shear modulus, t_1, t_2, and t_c are the thicknesses, e is the position of the neutral line, d is the distance between the center line of the steel and the high impact polystyrene beam, and z is the position of the reference axis.

According to Figure 1 and the theory of sandwich beams [Zenkert 1997]

$$e=\frac{E_1t_1\left(\frac{t_1}{2}+t_c+\frac{t_2}{2}\right)+E_ct_c\left(\frac{t_c}{2}+\frac{t_2}{2}\right)}{E_1t_1+E_ct_c+E_2t_2},\qquad d=t_c+\frac{t_1}{2}+\frac{t_2}{2},$$

$$D=\frac{E_1t_1^3}{12}+\frac{E_2t_2^3}{12}+\frac{E_ct_c^3}{12}+E_1t_1(d-e)^2+E_2t_2e^2+E_ct_c\left(\frac{t_c+t_2}{2}-e\right)^2,\quad \rho^*=\rho_1t_1+\rho_2t_2+\rho_ct_c,$$

$$\Re=\frac{\rho_1t_1^3}{12}+\frac{\rho_2t_2^3}{12}+\frac{\rho_ct_c^3}{12}+\rho_1t_1(d-e)^2+\rho_2t_2e^2+\rho_ct_c\left(\frac{t_c+t_2}{2}-e\right)^2,\qquad S=\frac{G_cd^2}{t_c}.$$

Making $w=w(x,t)$ a harmonic function, it is possible to admit that $w(x,t)=W(x)\,e^{i\omega t}$. Substituting this $w(x,t)$ into Equation (1) we obtain

$$D\frac{\partial^4 W}{\partial x^4}-\rho^*\omega^2W(x)-\frac{\rho^*}{S}\left(-D\omega^2\frac{\partial^2 W}{\partial x^2}-\Re\omega^4W(x)\right)+\Re\omega^2\frac{\partial^2 W}{\partial x^2}=f(x). \tag{2}$$

The exact solution $W(x)$ needs to satisfy Equation (2) at every point x, and in general is unknown. To overcome this problem the approximate solution $\tilde{W}(x)$ is used. This approximate solution is interpolated over a finite element, see Figure 1, with 2 nodes, according to the expression $W(x)\cong\tilde{W}(x)=[\phi]\,\{q\}$, where $[\phi(x)]$ is the shape function matrix (1×4) and the four $\phi_j(x)$ are the well known Hermitian interpolation functions [Cook et al. 1989] with C^1 continuity. The vector $\{q\}$ is the generalized displacement

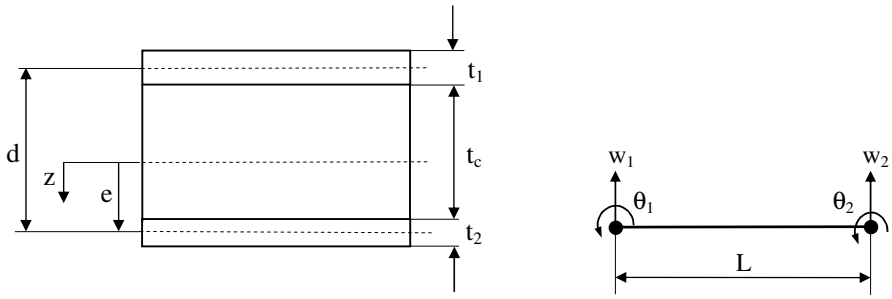

Figure 1. Sandwich beam geometric parameters (left) and finite element degrees of freedom (right).

vector, $\{q\} = \{w_1, \theta_1, w_2, \theta_2\}^t$ where w_i denotes the nodal displacement and θ_i is the rotation at element node i.

Substituting the approximate solution into Equation (2) introduces an residual error, $E(x, \omega)$, which is minimized using the Galerkin weighted residual method. In mathematical terms, the residual error is made orthogonal to the weight functions

$$\int_0^L [\phi]^t \left(D \frac{\partial^4 \tilde{W}}{\partial x^4} - \rho^* \omega^2 \tilde{W}(x) - \frac{\rho^*}{S} \left(-D\omega^2 \frac{\partial^2 \tilde{W}}{\partial x^2} - \Re \omega^4 \tilde{W}(x) \right) + \Re \omega^2 \frac{\partial^2 \tilde{W}}{\partial x^2} - f(x) \right) dx = 0, \quad (3)$$

where L is the element length.

Substituting the shape functions into Equation (3) obtains the standard finite element equation

$$[K_e(\omega)]\{q\} = \{F\},$$

where

$$[K_e(\omega)] = D[K] + \omega^2 \left[-\rho^*[M] + \left(\frac{\rho^* D}{S} + \Re \right) [K_\sigma] \right] + \omega^4 \frac{\rho^* \Re}{S} [M],$$

$$[K] = \frac{1}{L^3} \begin{bmatrix} 12 & 6L & -12 & 6L \\ 6L & 4L^2 & -6L & 2L^2 \\ -12 & -6L & 12 & -6L \\ 6L & 2L^2 & -6L & 4L^2 \end{bmatrix}, \qquad [K_\sigma] = \frac{1}{30L} \begin{bmatrix} 36 & 3L & -36 & 3L \\ 3L & 4L^2 & -3L & -L^2 \\ -36 & -3L & 36 & -3L \\ 3L & -L^2 & -3L & 4L^2 \end{bmatrix},$$

$$[M] = \frac{l}{420} \begin{bmatrix} 156 & 22L & 54 & -13L \\ 22L & 4L^2 & 13L & -3L \\ 54 & 13L & 156 & -22L \\ -13L & -3L & -22L & 4L^2 \end{bmatrix}, \qquad \{F\} = \int_0^L [\phi]^T f(x) dx.$$

3. Numerical estimation methods

To approximate the experimental and numeric FRF data, the predictor-corrector updating technique [Grafe 1998] based on two correlation coefficients (shape and amplitude) and their sensitivities can

be used. In this work, only the amplitude correlation coefficient is used. This coefficient is defined as

$$\chi_a(\omega_k) = \frac{2|\{H_X(\omega_k)\}^T\{H_A(\omega_k)\}|}{(\{H_X(\omega_k)\}^T\{H_X(\omega_k)\}) + (\{H_A(\omega_k)\}^T\{H_A(\omega_k)\})},$$

where $H_X(\omega_k)$ and $H_A(\omega_k)$ are the measured and predicted response vectors at matching excitation-response locations.

The corresponding sensitivity is

$$\frac{\partial \chi_a(\omega_k)}{\partial \varphi} = 2\frac{\partial|\{H_x\}^T\{H_A\}|}{\partial \varphi}\frac{(\{H_X\}^T\{H_X\}+\{H_A\}^T\{H_A\})}{(\{H_X\}^T\{H_X\}+\{H_A\}^T\{H_A\})^2} - 2\frac{\partial(\{H_A\}^T\{H_A\})}{\partial \varphi}\frac{|\{H_x\}^T\{H_A\}|}{(\{H_X\}^T\{H_X\}+\{H_A\}^T\{H_A\})^2}.$$

It is therefore proposed to make use of $\chi_a(\omega_k)$ and its sensitivity in a combined manner to improve the overall level of correlation. Based on a truncated Taylor series expansion, one can therefore write one equation for frequency point ω_k as

$$\{1-\chi_a(\omega_k)\} = \left[\frac{\partial \chi_a(\omega_k)}{\partial \varphi_1}\ \frac{\partial \chi_a(\omega_k)}{\partial \varphi_2}\ \cdots\ \frac{\partial \chi_a(\omega_k)}{\partial \varphi_{N_\varphi}}\right]_{1\times N_\varphi}\{\Delta\varphi\}, \tag{4}$$

where N_φ is the number of updating parameters $\{\varphi_1, \varphi_2, \ldots, \varphi_N\}$ and Equation (4) is recognized to be in the standard form of sensitivity based model updating formulations $\{\varepsilon\} = [S]\{\Delta\varphi\}$, where $\{\Delta\varphi\}$ is the change in design parameters of the finite element model.

An extended weighted least square approach is proposed which minimizes

$$J(\{\varphi\}) = \{\varepsilon\}^T\left[W_f\right]\{\varepsilon\} + \{\Delta\varphi\}^T\left[W_\varphi\right]\{\Delta\varphi\}, \tag{5}$$

where $\left[W_f\right]$ and $\left[W_\varphi\right]$ are diagonal weighting matrices for the frequency points and updating parameters respectively (see [Grafe 1998] for more details).

Another update method used in this work is the GA method. This method is widely used and is based on the evolutionary biological process [Chang 2006]; the GA parameters used in this application are: mutation rate = 0.02, population size = 50, and number of generations = 5000. The objective function is defined by

$$f = \sum_{i=1}^{np}|\mathrm{FRF}_{\mathrm{exp}} - \mathrm{FRF}_{\mathrm{FEM}}|, \tag{6}$$

where $\mathrm{FRF}_{\mathrm{exp}}$ is the experimental FRF obtained with laser transducer or accelerometer, $\mathrm{FRF}_{\mathrm{FEM}}$ is the numeric FRF and np is the number of experimental points (np varies according the system and frequency range). Equation (6) is used as a fitness function. The impulsive data were collected using a frequency range varying from 0 to 400 Hz and a frequency increment $\Delta\omega = 0.25$ Hz.

The numeric FRF is obtained using frequency sweeping in the range of interest with the same increment as the measurements. The final finite elements system of equations is solved for each frequency, and two procedures are used to specify the boundary condition and the force vector:

(a) When the FRF is obtained using the impact hammer, the force vector is calculated using unitary force applied in the excitation node, and the clamped boundary condition is prescribed for the fixed base node.

(b) When the FRF is obtained using base excitation (a shaker) and the measurements are made with a laser transducer, the force vector is null and the boundary conditions for the fixed base node are the measured displacement with null rotation.

4. Static characterization

This section shows the experimental procedure used to determine the material's mechanical properties, Young and shear moduli, and the density of the components of the sandwich beam. The elastic properties were obtained through tension and torsion tests. The shear modulus G_c of the polyurethane rigid foam core was determined with a torsion test using a prismatic specimen with a rectangular section, and the Young's moduli of the steel and high impact polystyrene were determined using conventional tension tests.

4.1. ***Polyurethane rigid foam core.*** Due to the difficulty of adapting the specimen for use in the conventional testing machines (for torsion and/or tension tests) a special pure torsion device test was projected to evaluate the shear modulus G of the core.

For pure torsion the relative angle of twist for a prismatic bar is

$$\theta = \frac{TL}{GJ},$$

where T is the torque, L is the length (as a relative position) and J is the polar area moment of inertia.

For a rectangular section with dimensions d and t with $d \geq t$ the polar area moment of inertia J is given by [Boresi and Chong 1999]

$$J = K_1 \frac{d \times t^3}{3},$$

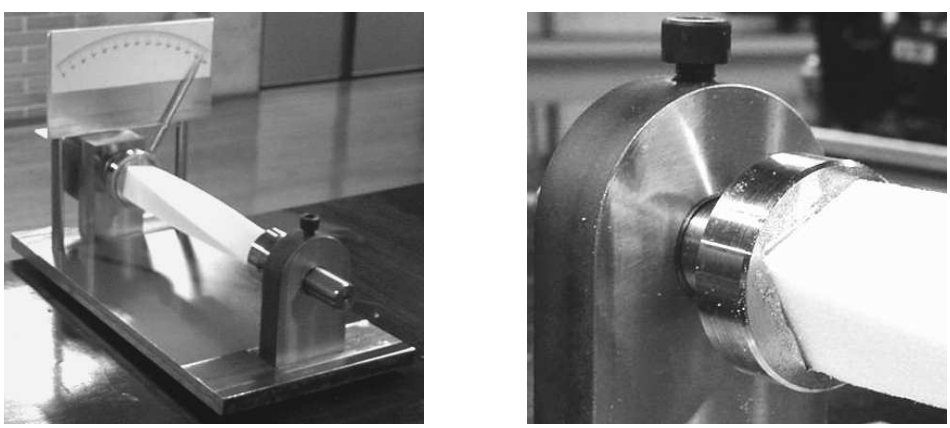

Figure 2. Special device for torsion test of the polyurethane rigid foam core (left) and the sample inserted in fixed extremity (right).

where

$$K_1 = 1 - \frac{192}{\pi^5}\frac{t}{d}\sum_{n=0,1,2,\ldots}\frac{1}{(2n+1)^5}\tanh\left(\frac{2n+1}{2}\frac{d}{t}\pi\right).$$

For $d = t$, using 10 terms in the series, $K_1 \cong 0.422$ and the expression for the angle of twist reduces to

$$\theta = \frac{T \times L}{G \times d \times t^3 \times 0.14066}.$$

The specimen with dimensions of 30 mm × 30 mm × 250 mm is inserted with low interference at the fixed extremity (see Figure 2), and the external torque is applied on the other extremity (which is free to rotate) using a pulley and dead weight (see Figure 3).

A cursor was inserted as shown in Figures 2 and 3 to measure the twist angle using a calibrated disc in steps with 0.5 degree resolution. The external torque is applied using calibrated weights (see Figure 3) and the test is carried out varying the torque and making direct measurement of the twist angle.

The polyurethane rigid foam samples were extracted from the same cabinet to avoid variations due to different production conditions. The samples were obtained from the lateral refrigerator wall (a straight region, with less foaming faults and voids) and it was classified according to the quantity of superficial faults (see Figure 4). The goal of this classification was to evaluate the variation of the G value obtained with perfect samples and with superficial faults.

The tests were performed on 12 samples with torque increments of 0.02375 Nm in such a manner to produce an adequate twist angle variation. Table 1 shows the values of G, as well the average value and the variance. The average values of the shear modulus G of samples with superficial faults are greater than that of samples without faults. Usually the stiffness will be reduced if there are defects in the specimen. However, the variance is also greater for the samples with faults.

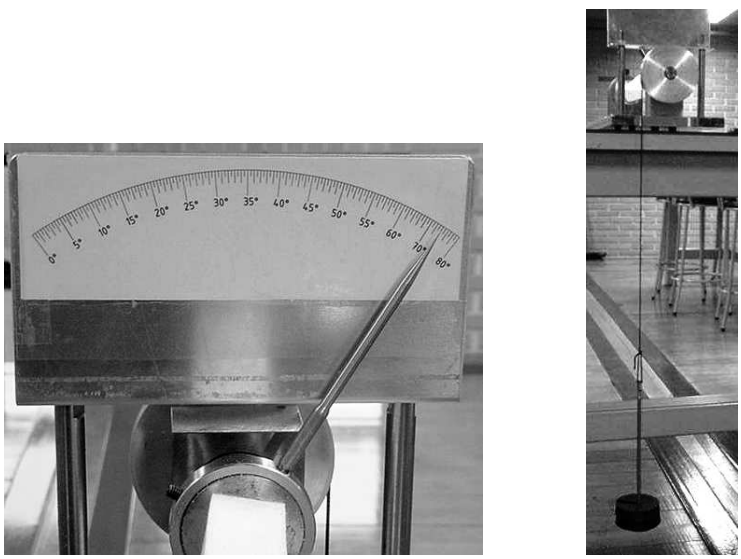

Figure 3. Free rotating end with calibrated disc (left) and torque application through calibrated weights (right).

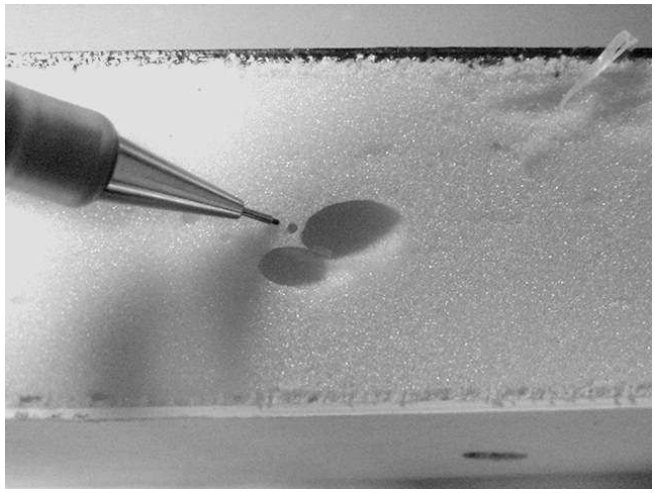

Figure 4. A sample with superficial faults.

Figure 5 shows a typical curve of the torque as a function of twist angle; it can be noticed that this relation is linear, with lower residue, as found in [Branner 1995]. Apparently the curve presents linear behavior. In the torsion test used to obtain the shear modulus G of the polyurethane rigid foam core, the twist angle can reach nearly 30 degrees. For such large rotation, the nonlinear effect may be dominant. The nonlinearity reduces the stiffness and lower G may be obtained.

Branner [1995] shows the dependence of the shear modulus G, as well as the elastic modulus E, on the specific material density. A precision weighing balance Scientech model SA210 was used, with resolution of 0.001 g. Table 2 shows the density values obtained for 12 samples (6 with and 6 without superficial faults).

4.2. ***Steel beam.*** The Young's modulus of the steel beam was determined using the procedures described in the technical norm [ASTM 2004].

Sample (without superficial faults)	G (MPa)	Sample (with superficial faults)	G (MPa)
1	1.977	1	2.423
2	2.015	2	1.896
3	2.215	3	1.935
4	2.045	4	2.205
5	2.091	5	2.496
6	2.054	6	2.152
Average value = 2.066 MPa Variance = 0.082 MPa		Average value = 2.184 MPa Variance = 0.245 MPa	

Table 1. Experimental shear modulus.

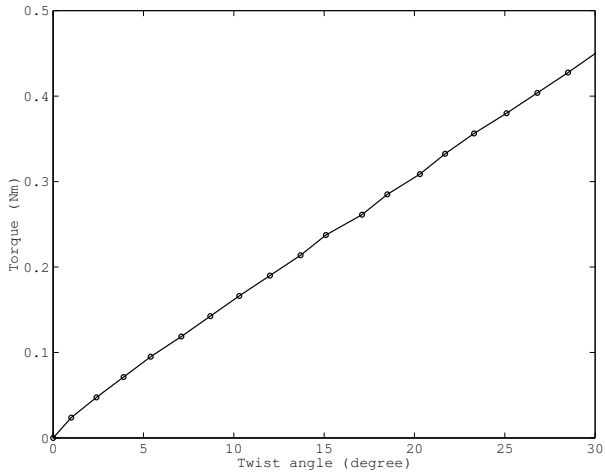

Figure 5. Twist angle versus applied torque.

As a result of the stress-strain test of the steel sample, a correlation between applied force and resultant deformations was obtained. The Young's modulus can be obtained from

$$E = \frac{P}{\varepsilon A},$$

where P is the applied load (in N), A is the transversal section area (in m^2), and ε is the longitudinal deformation (nondimensional).

The value of the Young's modulus obtained was 209.6 GPa, and Figure 6 shows the variation of the applied force and the strain.

4.3. ***High impact polystyrene.*** The characterization of the high impact polystyrene is performed using the procedures described in the technical norm [ASTM 2003] for plastics tensile testing.

Sample (without superficial faults)	Density (kg/m^3)	Sample (with superficial faults)	Density(kg/m^3)
1	28.400	1	29.111
2	28.876	2	28.573
3	28.769	3	28.262
4	28.751	4	29.280
5	28.369	5	29.111
6	28.329	6	29.671
Average value 28.582 kg/m^3 Variance 0.242 kg/m^3		Average value 29.002 kg/m^3 Variance 0.506 kg/m^3	

Table 2. Polyurethane rigid foam core density.

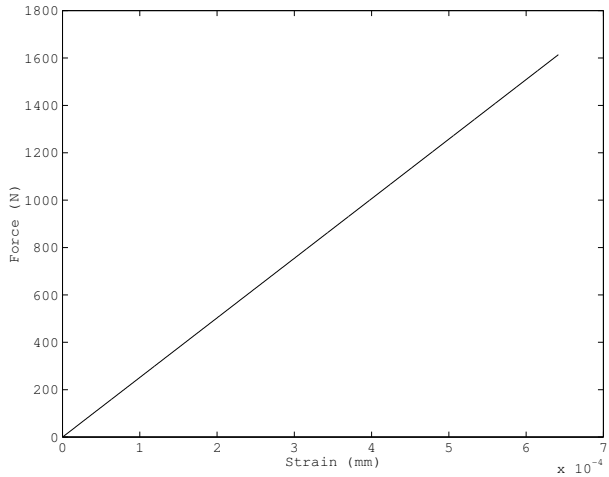

Figure 6. Strain versus applied force.

Five tests were carried out using a universal tensile testing machine EMIC with load cell capacity of 2000 N and test speed of 5 mm/min. The Young's modulus was obtained through the angular coefficient of the linear range of the stress-strain curve (see Figure 7).

Table 3 shows the Young's modulus values obtained from the five samples, the average value, and the variance.

The technical norm [ASTM 2000] describes the standard test methods for density and specific gravity (or relative density) of plastics by displacement. The body mass is first measured in the atmosphere. After this step the body is immersed in a liquid and the apparent mass is measured. After few manipulations the plastic density is obtained. Six samples were tested and the results are shown in Table 4.

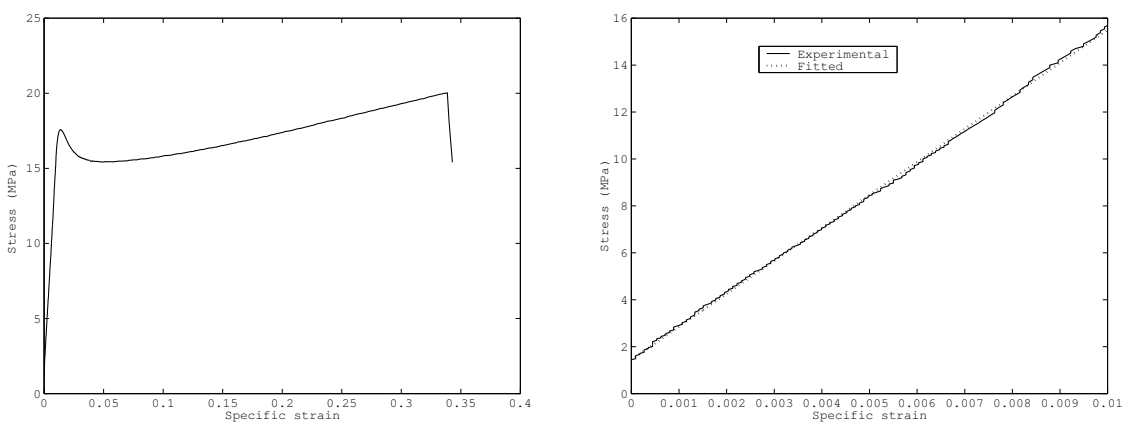

Figure 7. Specific strain versus stress (left) and adjusted curve of specific strain versus stress (right).

Sample	Young's modulus (GPa)
1	1.392
2	1.388
3	1.439
4	1.399
5	1.409
Average value 1.405 GPa Variance 0.018 GPa	

Table 3. Young's modulus of the PSAI.

5. Dynamic characterization

The experimental sample of the sandwich beam made with the association of hot rolled steel, polyurethane rigid foam, and high impact polystyrene is shown in Figure 8. The thicknesses of the steel, polyurethane, and polystyrene are 0.6 mm, 38.25 mm, and 1.25 mm, respectively, and the beam width is 39.18 mm.

The experimental data are obtained using the impact hammer and the four accelerometers displaced along the sample ($A1$, $A2$, $A3$, and $A4$). Figure 9 shows the FRF curves of the four accelerometers. The impact force was applied in the position of the accelerometer $A2$ on the steel side.

The rational fraction polynomial [Maia et al. 1997] method was used to estimate the damping ratio, ξ, and the natural frequencies, ω, of the first three mode shapes. The fourth mode was not considered due to poor signal to noise ratio.

Table 5 shows the values of these parameters for the four accelerometers. The position of the accelerometer $A3$ is near the nodal point of the second mode shape. This justifies the results suppressed in Table 5.

To validate the mathematical model of the sandwich beam it was attempted to estimate separately some physical parameters of the system, namely the shear modulus and the loss factor of the polyurethane rigid foam, and the Young's modulus and the loss factor of the high impact polystyrene.

Sample	Density (kg/m^3)
1	1059.6
2	1069.1
3	1060.1
4	1059.1
5	1060.3
6	1062.8
Average value 1061.9 kg/m^3 Variance 3.8 kg/m^3	

Table 4. Density of the PSAI.

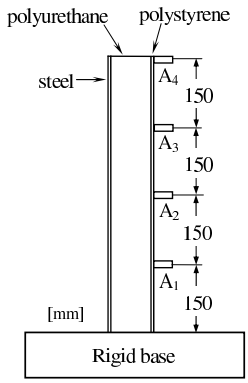

Figure 8. Sandwich beam.

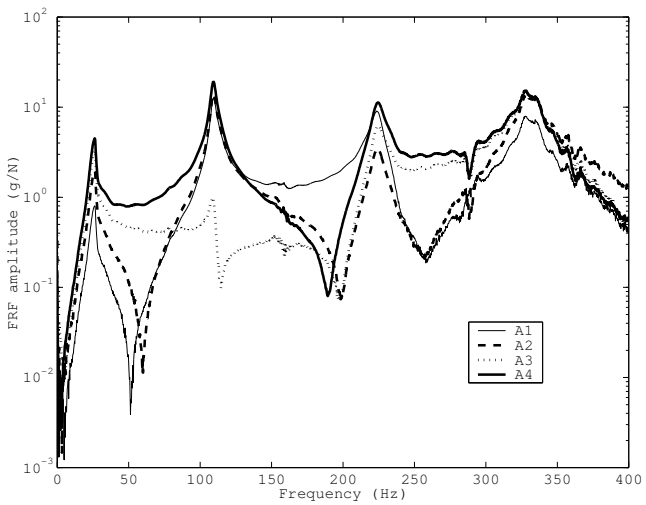

Figure 9. FRF curves of the four accelerometers.

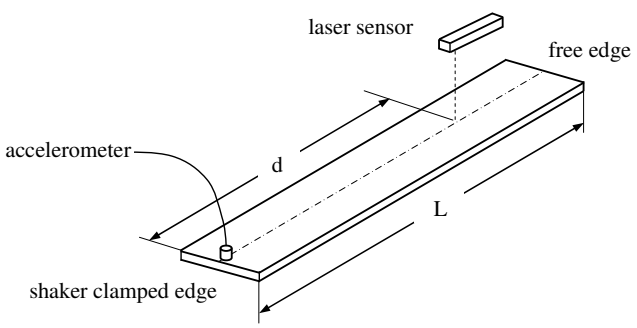

Figure 10. Experimental specimen of cantilever beam with position sensor.

	Accelerometers							
	A1		A2		A3		A4	
Mode shape	ω (Hz)	ξ	ω (Hz)	ξ	ω (Hz)	ξ	ω (Hz)	ξ
1	25.42	0.050	25.39	0.050	25.33	0.052	25.32	0.053
2	109.41	0.0171	109.45	0.0165	–	–	109.39	0.0167
3	223.97	0.0154	224.00	0.0152	224.05	0.0159	224.18	0.0157

Table 5. Experimental damping ratio and natural frequencies.

The loss factor η was estimated considering the complex Young's modulus $E^* = E(1 + j\eta)$. To obtain initial values of these parameters separate studies were conducted on the polyurethane rigid foam and the high impact polystyrene. The first approximation of the loss factor was $\eta = \xi \cong 0.05$ (the damping ratio of the first mode according Table 5).

Figure 10 shows the experimental specimen for the high impact polystyrene and polyurethane rigid foam cantilever beam. The high impact polystyrene beam dimensions and material property are length, $L = 0.145$ m, width $= 0.02$ m, thickness $= 0.0018$ m, and density $\rho = 1060\,\text{kg/m}^3$. The mini shaker (B&K model 4810) was used in the sweep sine test with the frequency range varied from 10 to 400 Hz with an increment of 2.5 Hz (157 points). One accelerometer (PCB model 353B18) and one laser velocity transducer (B&K model 3544) were used to collect the vibration data. The accelerometer was placed at the base excitation point (the shaker) and the laser sensor at the position $d = 0.135$ m. Figure 11 shows the experimental and estimated curves of the velocity/acceleration ratio PVA (velocity/base acceleration). The parameters were estimated using the genetic algorithm, and the objective function was defined using the difference between the values of the experimental and numeric PVA. The parameters updated are the Young's modulus and the loss factor of the high impact polystyrene. The optimal values found are shown in Table 6.

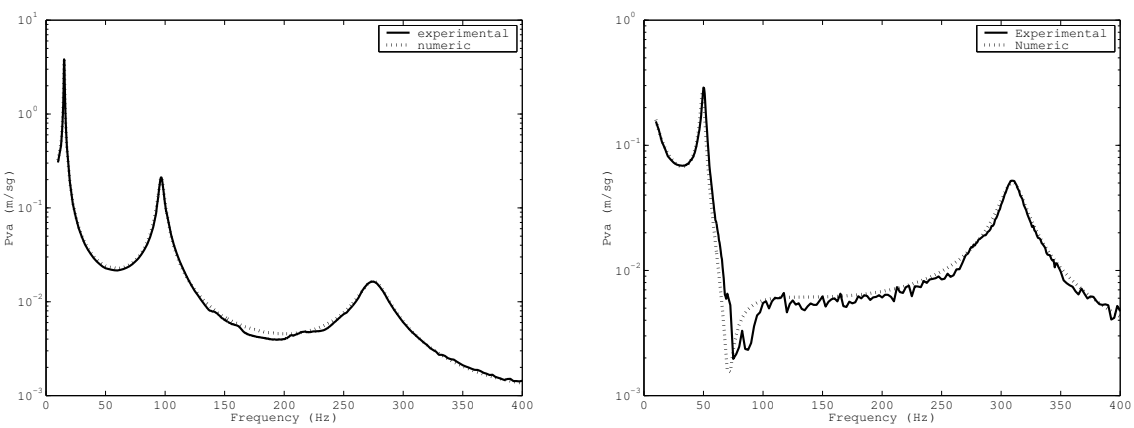

Figure 11. PVA curves of the high impact polystyrene cantilever beam (left) and the polyurethane rigid foam cantilever beam right.

Frequency range (Hz)	E (GPa)	η
10.0 – 57.5	1.3350	0.0385
57.5 – 177.5	1.3725	0.0450
177.5 – 400.0	1.4150	0.0805

Table 6. Optimal parameters.

Frequency range (Hz)	G (MPa)	η
10.0 – 150.0	2.6497	0.0575
150.0 – 400.0	2.5498	0.0625

Table 7. Optimal parameters.

The polyurethane rigid foam cantilever beam dimensions and material property are length, $L = 0.225$ m, width $= 0.03$ m, thickness $= 0.03$ m, and density $\rho = 29\,\text{kg/m}^3$. The laser sensor position is $d = 0.1125$ m. The mini shaker was used in the sweep sine test, with the frequency range varying from 10 to 400 Hz with an increment of 2.5 Hz (157 points). Figure 11 shows the experimental and the estimated curves of the velocity/acceleration ratio PVA. The parameters updated are the shear modulus and the loss factor of the polyurethane rigid foam. The optimal values found for these parameters are shown in Table 7. As mentioned by Backström [2006], the elasticity modulus of the core does not have significant influence on the dynamics of typical beams, and is assumed to be related to the core shear modulus by the isotropic relation $E_c = 2(1+\nu)G_c$, where ν is Poisson's ratio. Since the eigenfrequencies of the beam are not sensitive the value of ν, and as G_c is known directly, ν is set to a default value of $\nu = 0.3$. Thus, by defining an error function describing the proximity of the calculated curve of PVA to the measured, the optimal values of G_c are found by minimization.

Figure 11 shows good agreement between the estimated and experimental curves, even near the resonances.

The physical parameters of the cantilevered sandwich beam shown in Figure 8 were estimated using the amplitude correlation coefficient (ACC) and GA. The frequency range was varied from 10 to 250 Hz (961 points, $\Delta\omega = 0.25$ Hz), chosen for the good signal to noise ratio. Figure 12 shows the experimental and numeric (estimated) FRF curves for the sandwich beam. The curves obtained using ACC and GA methods are practically superposed, and the optimal parameter values found with these methods are shown in Table 8.

		High impact polystyrene		Polyurethane rigid foam	
Method	Frequency range (Hz)	E (GPa)	η	G (MPa)	η
GA	10 – 250	1.5830	0.0446	3.2874	0.0645
ACC	10 – 250	1.5800	0.0471	3.2917	0.0635

Table 8. Optimal parameters.

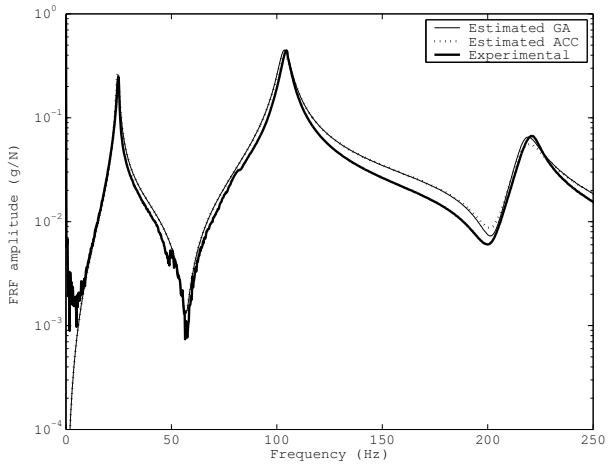

Figure 12. Experimental and estimated FRF curves.

6. Conclusions

Two methods, the genetic algorithm and the amplitude correlation coefficient methods, were used to update the values of physical parameters of mathematical models of a sandwich beam made with the association of hot rolled steel, polyurethane rigid foam, and high impact polystyrene as used for the assembly of household refrigerators and food freezers.

The physical parameters estimated were the shear modulus and the loss factor of the polyurethane rigid foam, and the Young's modulus and loss factor of the high impact polystyrene.

Both methods, the genetic algorithm and the amplitude correlation coefficient, presented good results when it compared to the estimated and the experimental FRF curves.

The genetic algorithm method does not use derivatives, thus it is a good estimated method even for the resonance region.

The amplitude correlation coefficient method uses derivatives, but even so it was possible to obtain good estimation of the parameters near the resonance region.

It was verified that the parameters are frequency dependent. The values found with a conventional, static, test are good approximations for the initial updated methods' starting point.

The static and dynamic tests yielded about the same, 1.4 GPa, for the elastic modulus of the high impact polystyrene. There is some discrepancy for the polyurethane rigid foam; the static test value is about 2.1 MPa, while the dynamic test value is about 2.5 MPa. Pritz [2004] demonstrated mathematically and verified experimentally that the modulus of elasticity of polyurethane rigid foam increases with the increase of the frequency. Therefore the results of this work are in accordance with the data of the literature.

The estimated parameters for the sandwich beam components are greater than the values estimated and measured for the individual (separated) samples. For sandwich beam samples the estimated Young's modulus of the high impact polystyrene was 1.58 GPa, and the estimated shear modulus of the polyurethane rigid foam was 3.29 MPa. The loss factor of the materials varied from 0.04 to 0.06. Some reasons for

the variations of the values between the static and dynamic tests can be associated with the compacting pressure, the glue between the layers, and imperfections in the foam core layer.

References

[ASTM 2000] "Standard test methods for density and specific gravity (relative density) of plastics by displacement", Technical report ASTM D792-00, 2000, Available at http://www.techstreet.com/cgi-bin/basket?action=add&item_id=3343161. 6 pages.

[ASTM 2003] "Standard test method for tensile properties of plastics", Technical report ASTM D638-03, 2003, Available at http://www.techstreet.com/cgi-bin/detail?product_id=1149803. 15 pages.

[ASTM 2004] "Standard test methods for tension testing of metallic materials [metric]", Technical report ASTM E8M-04, ASTM International, 2004, Available at http://www.techstreet.com/cgi-bin/basket?action=add&item_id=3644558. 24 pages.

[Backström 2006] D. Backström, *Vibration of sandwich beams*, Doctoral Thesis, Kungliga Tekniska Högskolan, Stockholm, 2006, Available at http://www.diva-portal.org/diva/getDocument?urn_nbn_se_kth_diva-4030-2__ful% ltext.pdf.

[Backström and Nilsson 2007] D. Backström and A. C. Nilsson, "Modelling the vibration of sandwich beams using frequency-dependent parameters", *J. Sound Vib.* **300**:3-5 (2007), 589–611.

[Boresi and Chong 1999] A. P. Boresi and K. P. Chong, *Elasticity in engineering mechanics*, 2nd ed., Wiley-Interscience, New York, 1999.

[Branner 1995] K. Branner, *Capacity and lifetime of foam core sandwich structures*, Doctoral Dissertation, Technical University of Denmark, Lyngby, Denmark, 1995.

[Caracciolo et al. 2004] R. Caracciolo, A. Gasparetto, and M. Giovagnoni, "An experimental technique for complete dynamic characterization of a viscoelastic material", *J. Sound Vib.* **272**:3-5 (2004), 1013–1032.

[Chang 2006] W.-D. Chang, "An improved real-coded genetic algorithm for parameters estimation of nonlinear systems", *Mech. Syst. Signal Process.* **20**:1 (2006), 236–246.

[Cook et al. 1989] R. D. Cook, D. S. Malkus, and M. E. Plesha, *Concepts and applications of finite element analysis*, 3rd ed., John Wiley & Sons, New York, 1989.

[Grafe 1998] H. Grafe, *Model updating structural dynamics models using measured response functions*, Ph.D. Thesis, Imperial College of Science, Technology & Medicine, Departament of Mechanical Engineering, London, 1998.

[Kim and Kreider 2006] S. Kim and K. L. Kreider, "Parameter identification for nonlinear elastic and viscoelastic plates", *Appl. Numer. Math.* **56**:12 (2006), 1538–1544.

[Maia et al. 1997] N. M. M. Maia and J. M. M. Silva (editors), *Theoretical and experimental modal analysis*, John Wiley & Sons Inc., New York, 1997.

[Ohkami and Swoboda 1999] T. Ohkami and G. Swoboda, "Parameter identification of viscoelastic materials", *Comput. Geotech.* **24**:4 (1999), 279–295.

[Park 2005] J. Park, "Transfer function methods to measure dynamic mechanical properties of complex structures", *J. Sound Vib.* **288**:1-2 (2005), 57–79.

[Pintelon et al. 2004] R. Pintelon, P. Guillaume, S. Vanlanduit, K. Belder, and Y. Rolain, "Identification of Young's modulus from broadband modal analysis experiments", *Mech. Syst. Signal Process.* **18**:4 (2004), 699–726.

[Pritz 2004] T. Pritz, "Frequency power law of material damping", *Appl. Acoust.* **65**:11 (2004), 1027–1036.

[Shi et al. 2006] Y. Shi, H. Sol, and H. Hua, "Material parameter identification of sandwich beams by an inverse method", *J. Sound Vib.* **290**:3-5 (2006), 1234–1255.

[Singh et al. 2003] R. Singh, P. Davies, and A. K. Bajaj, "Estimation of the dynamical properties of polyurethane foam through use of Prony series", *J. Sound Vib.* **264**:5 (2003), 1005–1043.

[Tavallaey 2001] S. S. Tavallaey, *Wave propagation in sandwich structures*, Doctoral Dissertation, Marcus Wallenberg Laboratory, Stockholm, 2001, Available at www.diva-portal.org/diva/getDocument?urn_nbn_se_kth_diva-3088-2__fulltext.pdf.

[Yang et al. 2005] W.-P. Yang, L.-W. Chen, and C.-C. Wang, "Vibration and dynamic stability of a traveling sandwich beam", *J. Sound Vib.* **285**:3 (2005), 597–614.

[Zenkert 1997] D. Zenkert, *Introduction to sandwich construction*, Engineering Materials Advisory Services, Cradley Heath, UK, 1997.

Received 18 Jun 2007. Revised 4 Sep 2007. Accepted 18 Sep 2007.

NILSON BARBIERI: nilson.barbieri@pucpr.br
Pontifícia Universidade Católica do Paraná, Programa de Pós-Graduação em Engenharia Mecânica, Rua Imaculada Conceição, 1155, Prado Velho, 80215-901 Curitiba, Paraná, Brazil

RENATO BARBIERI: renato.barbieri@pucpr.br
Pontifícia Universidade Católica do Paraná, Programa de Pós-Graduação em Engenharia Mecânica, Rua Imaculada Conceição, 1155, Prado Velho, 80215-901, Curitiba, Paraná, Brazil

LUIZ CARLOS WINIKES: luiz.winikes@ig.com.br
Pontifícia Universidade Católica do Paraná, Programa de Pós-Graduação em Engenharia Mecânica, Rua Imaculada Conceição, 1155, Prado Velho, 80215-901 Curitiba, Paraná, Brazil

LUIS FERNANDO ORESTEN: luis-fernando.oresten@electrolux.com.br
Pontifícia Universidade Católica do Paraná, Programa de Pós-Graduação em Engenharia Mecânica, Rua Imaculada Conceição, 1155, Prado Velho, 80215-901 Curitiba, Paraná, Brazil